Coupled spin- and charge-density waves in chromium alloys



1997 J. Phys.: Condens. Matter 9 3417

(http://iopscience.iop.org/0953-8984/9/16/013)

J. Phys.: Condens. Matter **9** (1997) 3417–3426. Printed in the UK PII: S0953-8984(97)75567-X

# Coupled spin- and charge-density waves in chromium alloys

X W Jiang†§ and R S Fishman‡

† Physics Department, North Dakota State University, Fargo, ND 58105-5566, USA

‡ Solid State Division, PO Box 2008, Oak Ridge National Laboratory, Oak Ridge, TN 37831-6032, USA

Received 20 June 1996, in final form 7 October 1996

**Abstract.** Both the spin- and charge-density waves in Cr alloys are produced by the Coulomb attraction between electrons and holes on two nested Fermi surfaces. The Coulomb interaction responsible for the charge-density wave increases the energy splitting between quasiparticles which are strongly and weakly bound to the spin-density wave. If the splitting is sufficiently large, the paramagnetic-to-commensurate transition becomes strongly first order, as observed in CrFe and CrSi alloys.

It is well known that the spin-density wave [1, 2] (SDW) of Cr alloys is produced by the Coulomb attraction $U$ between electrons and holes on almost perfectly nested [3] Fermi surfaces $a$ and $b$. Because the hole Fermi surface $b$ is slightly larger than the electron Fermi surface $a$, the SDW of pure Cr is incommensurate (I) with the bcc lattice. The nesting of the Fermi surfaces and the wavevectors $\boldsymbol{Q}'_{\pm}$ of the SDW can be controlled by shifting the chemical potential with doping. When the $a$ and $b$ Fermi surfaces are sufficiently close in size [4], the SDW becomes commensurate (C) with the lattice and $\boldsymbol{Q}'_{\pm} = \boldsymbol{G}/2$, where $\boldsymbol{G} = 4\pi\hat{\boldsymbol{z}}/a$ is a reciprocal-lattice vector. In the I phase, a charge-density wave (CDW) with wavevectors $2\boldsymbol{Q}'_{\pm}$ on either side of $\boldsymbol{G}$ is produced by the Coulomb attraction $U'$ between electrons and holes on the $b$ Fermi surface. In the C phase, however, the physical significance of $U'$ and the fate of the CDW have been unclear. We show that although the CCDW disappears, the Coulomb interaction $U'$ may be responsible for the strong first-order transition from the paramagnetic (P) phase to the C phase [1] observed in CrFe and CrSi alloys.

Both x-ray [5, 6] and neutron scattering [7, 8] measurements revealed the existence of a CDW in I Cr alloys over 20 years ago. The most recent and complete set of measurements on pure Cr using x-rays were performed by Hill *et al* [9]. If the wavevectors of the ISDW are $\boldsymbol{Q}'_{\pm} = (\boldsymbol{G}/2)(1 \pm \partial')$, then the wavevectors of the CDW are $2\boldsymbol{Q}'_{\pm} = \boldsymbol{G}(1 \pm \partial')$. While the SDW with order parameter $g$ drives the antiferromagnetic phase transition, the CDW with order parameter $\delta$ is itself driven [10] by the formation of the SDW.

To minimize the condensation free energy [4] on both sides of the two Fermi surfaces, the ordering wavevectors $\boldsymbol{Q}'_{\pm}$ of the SDW lie closer to $\boldsymbol{G}/2$ than the nesting wavevectors $\boldsymbol{Q}_{\pm} = (\boldsymbol{G}/2)(1 \pm \partial)$. The mismatch $\partial$ between the $a$ and $b$ Fermi surfaces can be controlled by doping with another transition metal: adding Mn, Fe, Re, or Ru raises the chemical potential and decreases $\partial$; adding V lowers the chemical potential and increases the mismatch

§ Current address: Center for Ceramic Research, Rutgers University, Piscataway, NJ 08855-0909, USA.

0953-8984/97/163417+10$19.50  

$\partial$. For pure Cr, $\partial \approx 0.05$, so the hole Fermi surface is only slightly larger than the electron surface. As $\partial$ decreases and the nesting improves, $\partial' < \partial$ also decreases until, for a small enough mismatch $\partial > 0$, the SDW becomes commensurate with $\partial' = 0$. Although domains of the ISDW may form along any of the three crystal axis, an ISDW along the $z$ axis can be selected by cooling the I alloy in a magnetic field in the $z$ direction.

Besides the nested $a$ and $b$ Fermi surfaces with the density of states $\rho_{eh}$, the band structure of Cr alloys also contains two other bands of electron balls and hole pockets [11, 12] which may be lumped together into an electron reservoir with density of states $\rho_r$ and power $\rho = \rho_r/\rho_{eh}$. If the electron reservoir is finite [13, 14], then the chemical potential will decrease and the mismatch $\partial$ will increase with the growth of the SDW. So a finite electron reservoir favours the I phase of the SDW.

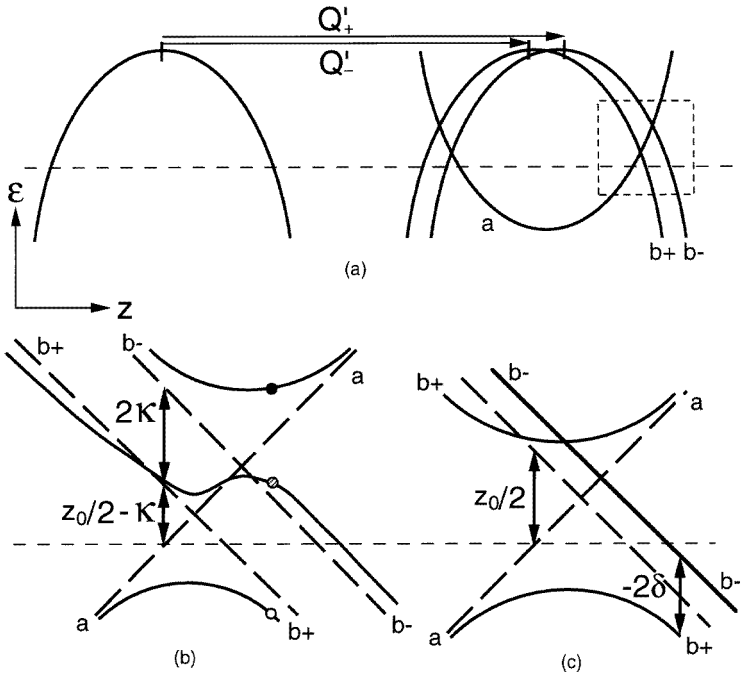


**Figure 1.** (a) The electron ($a$) and hole ($b$) energies translated by the SDW wavevectors $\boldsymbol{Q}'_{\pm}$. In (b) and (c), we expand the boxed region near the Fermi energy for the quasiparticle energies above (short-dashed lines) and below (solid lines) the Néel temperature for the I and C phases. In all three figures, the chemical potential is denoted by a horizontal dashed line.

In figure 1(a), the paramagnetic energies of band $b$ are shifted by the ordering wavectors $\boldsymbol{Q}'_{\pm}$. The linearized energies in the boxed region near the Fermi wavevector $k_F$ are then plotted as the dashed lines of figures 1(b) and 1(c) for the I and C phases, respectively. In all three figures, the chemical potential is denoted by a dashed horizontal line, and $z = v_F(\boldsymbol{k} \cdot \hat{\boldsymbol{n}} - k_F)$ measures the momentum difference from an octahedral face of the electron Fermi surface with normal $\hat{\boldsymbol{n}}$. Since the difference in size between the Fermi surfaces $a$ and $b$ is actually quite small, the Fermi velocities $v_F$ of the two surfaces are assumed to be equal. The paramagnetic energies are then specified by the parameters $z_0 = 4\pi\partial v_F/\sqrt{3}a$ and $\kappa = z_0\partial'/2\partial$. For pure Cr, $z_0 \approx 375$ meV and $\kappa \approx 150$ meV. While $z_0$ increases linearly with the V concentration, it decreases linearly with the concentration

of Mn, Fe, Re, or Ru. The second parameter, $\kappa$, measures the incommensurability of the SDW and vanishes for a C alloy. Another quantity which will appear shortly is the Néel temperature $T_N^* \approx 80$ meV of a perfectly nested Cr alloy with $z_0 = 0$ and $\kappa = 0$.

Quasiparticles with paramagnetic energies $\epsilon_{b+}(\boldsymbol{k}) = \epsilon_b(\boldsymbol{k} - \boldsymbol{Q}'_-)$ and $\epsilon_{b-}(\boldsymbol{k}) = \epsilon_b(\boldsymbol{k} - \boldsymbol{Q}'_+)$ are already indirectly coupled through the SDW with order parameter $g$. But a hole on band $b+$ and an electron on band $b-$ are also directly coupled by the Coulomb attraction [10] $U' > 0$, which produces a CDW with order parameter $\delta < 0$. Since the momenta of the $b\pm$ quasiparticles have been shifted by $\boldsymbol{Q}'_\mp$, the CDW carries momentum $\pm(\boldsymbol{Q}'_+ - \boldsymbol{Q}'_-) = 2\boldsymbol{Q}'_\pm - \boldsymbol{G}$ and may be considered the second harmonic [10] of the SDW. Although the CDW is driven by the SDW, we shall see that it affects the thermodynamics of Cr alloys in a highly nontrivial way.

Below the Néel temperature, the hybridized quasiparticle energies are obtained from the six-dimensional Green's function in band $\{a, b-, b+\}$ and spin space:

$$\mathbf{G}^{-1}(\boldsymbol{k}, \mathrm{i}\nu_l) = \begin{pmatrix} (\mathrm{i}\nu_l - \epsilon_a(\boldsymbol{k}))\mathbf{1} & -\mathbf{g}\mathrm{e}^{\mathrm{i}\phi_-} & -\mathbf{g}\mathrm{e}^{\mathrm{i}\phi_+} \\ -\mathbf{g}\mathrm{e}^{-\mathrm{i}\phi_-} & (\mathrm{i}\nu_l - \epsilon_{b-}(\boldsymbol{k}))\mathbf{1} & -\delta\mathbf{1}\mathrm{e}^{\mathrm{i}\psi} \\ -\mathbf{g}\mathrm{e}^{-\mathrm{i}\phi_+} & -\delta\mathbf{1}\mathrm{e}^{-\mathrm{i}\psi} & (\mathrm{i}\nu_l - \epsilon_{b+}(\boldsymbol{k}))\mathbf{1} \end{pmatrix} \tag{1}$$

where $\nu_l = (2l + 1)\pi T$. While the CDW order parameter $\mathbf{1}\delta$ is diagonal in spin space, the SDW order parameter is given by $\mathbf{g} = g\hat{\boldsymbol{m}} \cdot \boldsymbol{\sigma}$, where $\hat{\boldsymbol{m}}$ is the polarization direction of the SDW and $\boldsymbol{\sigma}$ are the Pauli matrices in spin space. To ensure that the SDW and CDW order parameters $g(T)$ and $\delta(T)$ are real, the $ab\pm$ and $b+b-$ matrix elements have been assigned phases $\phi_\pm$ and $\psi$.

The quasiparticle energies are solved from the condition $\mathrm{Det}\,\mathbf{G}^{-1}(\boldsymbol{k}, \epsilon) = 0$, which may be rewritten as

$$\begin{aligned} D(\boldsymbol{k}, \epsilon, g, \delta, \kappa) \equiv{}& (\epsilon - z)((\epsilon + z - z_0/2)^2 - \kappa^2 - \delta^2) \\ & - 2g^2(\epsilon + z - z_0/2 + \delta\cos(\psi - \theta)) = 0 \end{aligned} \tag{2}$$

with $\theta = \phi_+ - \phi_-$. Within the random-phase approximation, the self-consistent expressions for the SDW and CDW order parameters are given by equations (A1) and (A2) in the appendix. These two relations imply that $\psi = \theta$. For $k_z > 0$, the resulting hybridized energies are plotted as the solid curves of figure 1(b) and 1(c); for $k_z < 0$, the $b\pm$ indices must be reversed.

Because the $b$ Fermi surface is larger than the $a$ Fermi surface, there are more holes than electrons, and they cannot all be paired to electrons in the SDW. Since the mismatch between the paramagnetic C energies of figure 1(c) is $z_0/2$, the density of unpaired quasiparticle states is $\rho_{eh}z_0/4$, which increases linearly with the energy mismatch $z_0$ between the Fermi surfaces. For $k_z > 0$, the $b+$ quasiparticles are more strongly bound by the SDW than the $b-$ quasiparticles.

In the C phase with $\kappa = 0$, the hybridized energy $\epsilon_{b-} = -z + z_0/2 - \delta$ of the straight $b-$ band in figure 1(c) is displaced from its paramagnetic value solely by the Coulomb interaction $U'$. The $b-$ quasiparticles are then completely unbound from the SDW. As $U'$ and $-\delta$ increase, the energy splitting between the $b\pm$ bands increases and more of the unpaired holes transfer from the $b+$ to the $b-$ band. Consequently, the $ab+$ bands shift downward in energy and the $b-$ band shifts upwards. In the limit of large $|z|$, the splitting between the $b\pm$ bands tends to $-2\delta$.

In the I phase, the $b-$ quasiparticles are still weakly bound to the SDW. As $-\delta$ grows, the energy splitting between the $b+$ and $b-$ quasiparticles increases and it becomes increasingly favourable for $b-$ electrons on the central band to fill any $b+$ states vacated on the lower $ab+$ band. An ICDW is then produced by the Coulomb attraction $U' > 0$

between strongly bound $b+$ holes on the lower band and weakly bound $b-$ electrons on the central band. Suppose, for example, that enough energy is provided to break apart an electron–hole pair, drawn as the open and filled (solid or hatched) circles in figure 1(b). While the SDW is produced by the Coulomb attraction $U$ between the solid electron on the upper band and the hole on the lower band, the CDW is produced by the Coulomb attraction $U'$ between the hatched electron on the central band and the hole below it. Because the velocities of the hatched electron and hole have the same sign, the Coulomb interaction $U'$ cannot generate a CDW in the absence of a SDW. So for small values of $g$, the CDW order parameter $\delta$ is proportional to $-\rho_{eh}U'g^2/T_N^*$.

Starting with the Green's function of equation (1), the spin and charge distributions as derived in the appendix are given by

$$\boldsymbol{S}(\boldsymbol{r}) = -\frac{\overline{h}}{2\lambda} V\rho_{eh} g\hat{\boldsymbol{m}}|u(\boldsymbol{r})|^2 \cos\left(\frac{2\pi}{a}r_z - \phi_{av}\right)\cos\left(\frac{2\pi}{a}\partial' r_z - \frac{\theta}{2}\right) \tag{3}$$

$$\varrho(\boldsymbol{r}) = -\frac{1}{2\lambda'} V\rho_{eh}\delta|u(\boldsymbol{r})|^2 \cos\left(\frac{4\pi}{a}\partial' r_z - \psi\right) \tag{4}$$

where $\lambda = \rho_{eh}U/2$ and $\lambda' = \rho_{eh}U'/2$ are dimensionless coupling constants, $\phi_{av} = (\phi_+ + \phi_-)/2$, and $u(\boldsymbol{r})$ is a periodic Bloch function normalized to 1 in volume $V$. Since the Bloch functions of the d-band electrons are strongly peaked at the atomic sites, the maximum values of the spin and electron number at each of the $N$ sites in the I phase are $S_0 = (\overline{h}g/2\lambda)\cos\phi_{av}(V/N)\rho_{eh}$ and $\varrho_0 = -(\delta/2\lambda')(V/N)\rho_{eh}$. In terms of these I amplitudes, the spin and charge amplitudes in the C phase are $S_0\cos(\theta/2)$ and $\varrho_0\cos\psi$.

Because $\psi = \theta$, the ISDW and ICDW are in phase: the electron number $\varrho(\boldsymbol{r})$ is largest whenever the magnitude of the spin $|\boldsymbol{S}(\boldsymbol{r})|$ is a maximum, as shown in figures 2(a) and 2(b). For the CDW pictured in figure 2(b), black dots signify atomic sites with extra electronic density $\varrho(\boldsymbol{r}) > 0$ and white dots are atomic sites with deficit electrons $\varrho(\boldsymbol{r}) < 0$. The sizes of the dots scale with the magnitude of $\varrho(\boldsymbol{r})$. Notice that the CDW goes through two complete periods as the SDW goes through one. The phase relationship between the SDW and CDW agrees with the recent analysis of x-ray scattering data by Mori and Tsunoda [15].

Due to electron–phonon coupling, a strain wave [15, 16] is produced by the response of the atomic cores to the CDW. If the new atomic positions are given by $\boldsymbol{R} = \boldsymbol{R}_0 + \boldsymbol{\Delta}(\boldsymbol{R}_0)$, then the Bloch functions in equations (3) and (4) are shifted by the strain wave. The strain wave $\boldsymbol{\Delta}(\boldsymbol{R})$ has the same periodicity as the CDW and the same orientation as the ordering wavevectors. Since the strain-wave amplitude is proportional to the CDW amplitude, it also vanishes above $T_N$. However, Nakajima and Kurihara [16] have argued that the electron–phonon coupling in Cr is insufficient to generate a strain wave with the observed amplitude.

Of course, the ICDW of equation (4) carries no net charge. Notice that the ICDW involves the long-range modulation of the charge rather than a simple redistribution of the charge within each unit cell. While electrostatic energies would be expected to inhibit such a charge reordering [17], the strain wave acts to reduce the local electronic charge density by increasing the spacing [15] between atoms with excess electrons. With the density of states [18] $(V/N)\rho_{eh} = 2.4$ states Ryd$^{-1}$/atom, the ICDW amplitude $\varrho_0$ ranges [19] from 0.0054 ($\lambda' = 0.15$) to 0.0142 ($\lambda' = 0.4$) electrons per site. These estimates are close to those of Mori and Tsunoda [15], who used the asymmetry between the x-ray scattering intensities at $\boldsymbol{Q}'_{\pm}$ to distinguish the contributions of the CDW from the strain wave in pure Cr.

Unlike the ICDW, a CCDW with $\partial' = 0$ would carry a net charge of $\varrho_0\cos\theta$ at each atomic site. Conservation of charge among the nested Fermi surfaces and the reservoir bands

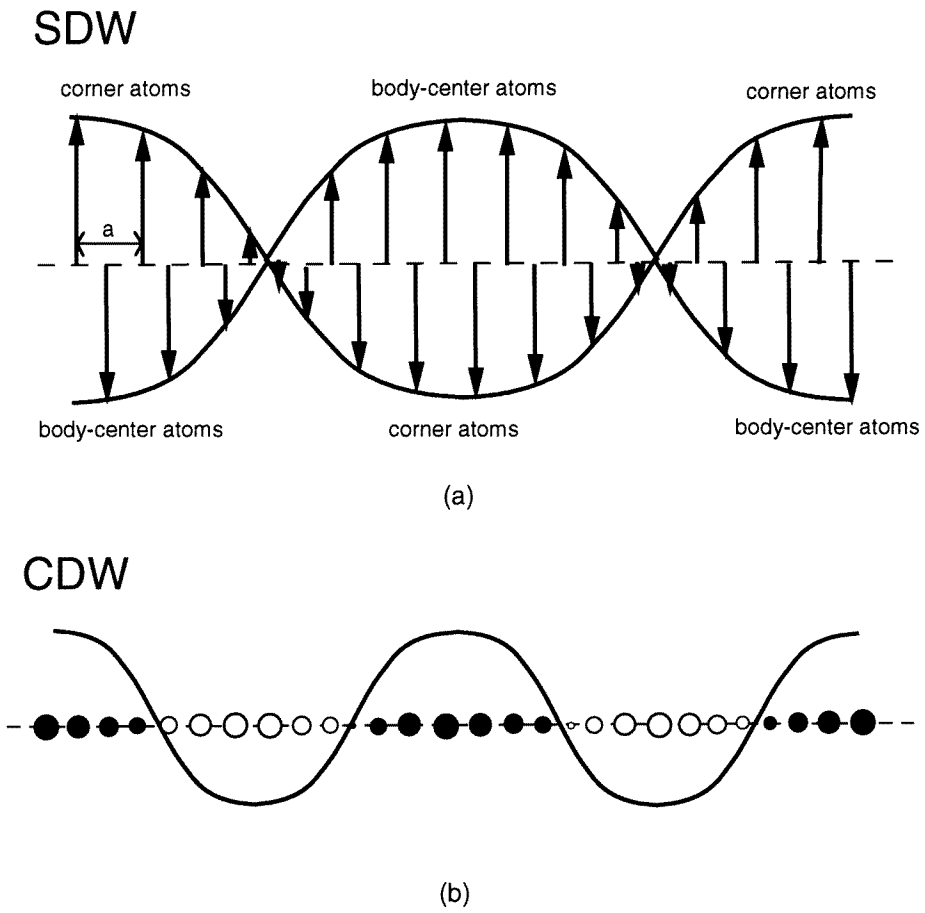


**Figure 2.** Plots of the (a) SDW $\boldsymbol{S}(\boldsymbol{r})$ and (b) CDW $\varrho(\boldsymbol{r})$. In the latter figure, black or white dots denote positive or negative electron numbers. For clarity, the SDW is drawn with a wavelength of $14a$, less than the wavelength of $24a$ for pure Cr.

[20] requires that this CCDW vanish. Therefore, $\cos\theta$ must vanish in the C phase and *the Coulomb attraction $U'$ only generates a CDW in the I phase.* As another consequence, the *rms* value of the spin will change continuously across a second-order IC transition, but the maximum spin will decrease from $S_0$ to $S_0/\sqrt{2}$.

After integrating the self-consistent equations for the SDW and CDW order parameters, we obtain the free-energy difference [20] between the paramagnetic and ordered states with an infinite electron reservoir:

$$\frac{1}{\rho_{eh}}\Delta F(g,\delta,\kappa) = \frac{1}{2\lambda}g^2 + \frac{1-2\lambda'}{4\lambda'}\delta^2 - \frac{T}{2V\rho_{eh}}\sum_{l,\boldsymbol{k}}\ln\left(\frac{D(\boldsymbol{k},\mathrm{i}\nu_l,g,\delta,\kappa)}{D(\boldsymbol{k},\mathrm{i}\nu_l,0,0,\kappa)}\right). \tag{5}$$

The stable solutions for the order parameters $g$ and $\delta$ as well as for the wavevector parameter $\kappa$ must minimize this free energy.

Because the shifted paramagnetic energies $\epsilon_{b\pm}(\boldsymbol{k}) = \epsilon_b(\boldsymbol{k} - \boldsymbol{G}/2)$ are identical in the C phase, a three-band model might seem unnecessary [10] and the physical significance of the Coulomb interaction $U'$ may be unclear. But even in the C phase, the $b\pm$ quasiparticles

are physically distinct: whereas the $b+$ quasiparticles (for $k_z > 0$) are bound to the SDW, the $b-$ quasiparticles are unbound. The direct Coulomb interaction $U'$ between the paired $b+$ holes and the unpaired $b-$ electrons requires the use of a three-band model even in the C phase. Since the density of unpaired $b-$ quasiparticle states is proportional to $\rho_{eh} z_0$, the three-band model can only be abandoned in the $z_0 \to 0$ limit of perfect nesting.

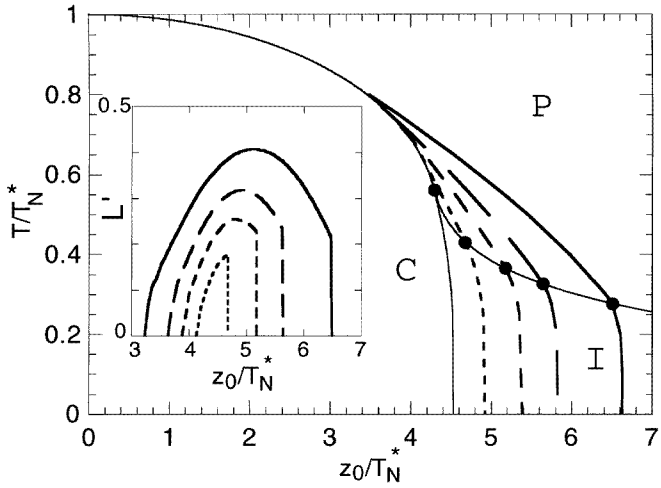


**Figure 3.** The phase diagram of Cr alloys with $\rho = \infty$ and $\lambda' = 0.4$ (solid line), 0.35 (long-dashed line), 0.30 (medium-dashed line), 0.20 (short-dashed line), and 0 (thin solid line). The triple points are indicated by the filled circles and the second-order paramagnetic phase boundary is denoted by a thin solid line. The inset shows the normalized latent heat $L'$ for the same parameters. The three different magnetic phases are labelled.

Our results for an infinite electron reservoir are presented in figure 3. Notice that the PI transition is always second order. By contrast, Young and Sokoloff [10] obtained a first-order PI transition above a threshold value [21] of $\lambda'$ after setting the SDW ordering wavevectors equal to the nesting wavevectors (equivalent to fixing $\partial' = \partial$ or $\kappa = z_0/2$). When the free energy $\Delta F$ is minimized with respect to $\partial'$ or $\kappa$, the I solutions near the first-order phase boundary are unstable. Rather, a nonzero $\lambda'$ always drives a first-order PC transition and pushes the triple point towards higher values of $z_0$. As $\lambda' \to 1/2$, the CDW becomes unstable and the I phase disappears. For $\lambda' > 1/2$, $\Delta F \to -\infty$ as $\delta \to -\infty$ and no physical solutions exist. The discontinuity of the slope $\mathrm{d}T_N/\mathrm{d}z_0$ at the triple point, which has been observed in all Cr alloys but never previously explained, is a natural consequence of this model.

The normalized and dimensionless latent heat $L' = L/\rho_{eh} T_N^{*2}$ of the first-order PC transition is plotted in the inset of figure 3. As observed in CrFe and CrSi alloys [1], the latent heat $L = T_N \, \partial \Delta F/\partial T|_{T_N^-}$ peaks to the left of the triple point. If $\rho_{eh} = 2.4$ states $\mathrm{Ryd}^{-1}$/atom, then fitting the observed maximum latent heat [1] of 12.6 J $\mathrm{mol}^{-1}$ for CrFe alloys yields $\lambda' \approx 0.135$.

When the electron reservoir is infinite, the CI transition is first order for any $\lambda' \geqslant 0$ and the PC transition is first order close to the triple point for any $\lambda' > 0$. As discussed elsewhere [20], a finite electron reservoir introduces a threshold value for $\lambda'$, below which the PC transition is second order for all $z_0$. Since a finite reservoir suppresses the latent heat $L'$, the estimate given above for $\lambda'$ in CrFe alloys is only a lower bound. Just as in

the absence of a CDW [14], a finite reservoir swings the CI phase boundary to the C side of the triple point and suppresses a first-order CI transition. By stabilizing the I solutions near the first-order phase boundary, the finite reservoir also drives the weak first-order PI transition observed [1] in pure Cr.

For CrMn, CrRe, or CrRu alloys, a first-order PC transition may be averted by the suppression of $\lambda'$ with the impurity concentration. Due to the small size of the electron reservoir, the CI transition is either weakly first order (CrMn) or second order (CrRe and CrRu).

Unlike other impurity atoms [1], Fe retains its localized magnetic moment [22, 23] within the Cr host below $T_N$. Because far fewer of its impurity electrons enter the conduction band, the triple point for CrFe alloys lies at a much higher concentration than for CrMn alloys: 2.4% Fe compared to 0.3% Mn. By enhancing the electron reservoir [24], the localized electrons on the Fe moments bend the first-order CI phase boundary to the I side of the triple point as in figure 3. Due to the indirect exchange of $b+$ holes and $b-$ electrons mediated by the paramagnetic Fe moments, the coupling $\lambda'$ may grow with the Fe concentration, thereby generating a large CDW in the I phase and producing a strong first-order PC transition into the C phase.

Unfortunately, such a simple picture cannot explain the strong first-order PC transition produced by Si impurities, which are nonmagnetic. Like the triple point of CrFe, the triple point of CrSi lies at a rather high impurity concentration of 1.3%. So, contrary to predictions from simple counting arguments [25], Si impurities also act as weak electron donors. Fawcett [26] has recently suggested that the effect of Si impurities may be produced by a volume expansion which reduces [1] the energy mismatch $z_0$. As for CrFe alloys, we believe that the strong first-order PC transition in CrSi alloys is also driven by the energy splitting between the bound and unbound quasiparticles.

While the CDW vanishes in the C phase, the growth of the CDW from the I side of the phase boundary should be straightforward to measure. As observed experimentally [9] and verified [20] by our model, the ratio $\varrho_0/S_0^2 \propto 1/(1-2\lambda')$ is almost independent of temperature and provides a direct measure of the coupling constant $\lambda'$. So low-temperature x-ray or neutron scattering measurements of $\varrho_0/S_0^2$ on a series of I $Cr_{1-x}A_x$ alloys can confirm that $\lambda'(x)$ grows with the Fe or Si concentration and decreases with the Mn, Re, or Ru concentration.

## Acknowledgments

One of us (RF) would like acknowledge support from the US Department of Energy under Contract No DE-FG06-94ER45519 and under Contract No DE-AC0586OR22464 with Lockheed Martin Energy Research Corporation. Useful conversations with H Alberts, E Fawcett, B Gaulin, B Larson, Y Tsunoda, V S Viswanath, S Werner, and especially with S H Liu are also gratefully acknowledged.

## Appendix

Within the random-phase approximation, the self-consistent relations for the spin- and charge-density-wave order parameters are

$$g\hat{\boldsymbol{m}}\cdot\boldsymbol{\sigma}\mathrm{e}^{\mathrm{i}\phi_+} = -U\frac{T}{V}\sum_{\boldsymbol{k},l}\mathbf{G}^{ab+}(\boldsymbol{k},\mathrm{i}\nu_l)$$

$$= -U\frac{T}{2V}\sum_{\boldsymbol{k},l}\frac{2\mathrm{i}\nu_l - \epsilon_{b+}(\boldsymbol{k}) - \epsilon_{b-}(\boldsymbol{k}) + 2\delta\mathrm{e}^{\mathrm{i}(\psi-\theta)}}{D(g,\delta,\Lambda,\mathrm{i}\nu_l)}g\hat{\boldsymbol{m}}\cdot\boldsymbol{\sigma}\mathrm{e}^{\mathrm{i}\phi_+} \tag{A1}$$

$$\delta\mathbf{1}\mathrm{e}^{\mathrm{i}\psi} = -U'\frac{T}{V}\sum_{\boldsymbol{k},l}\mathbf{G}^{b+b-}(\boldsymbol{k},\mathrm{i}\nu_l) = -U'\frac{T}{V}\sum_{\boldsymbol{k},l}\frac{(\mathrm{i}\nu_l - \epsilon_a(\boldsymbol{k}))\delta\mathrm{e}^{\mathrm{i}\psi} + g^2\mathrm{e}^{\mathrm{i}\theta}}{D(g,\delta,\Lambda,\mathrm{i}\nu_l)}\mathbf{1}. \tag{A2}$$

The sum over $\boldsymbol{k}$ has been used to symmetrize equation (A1) over the two hemispheres with $k_z > 0$ and $k_z < 0$. These two expressions require $\psi = \theta$ (an additional $\pi$ can be absorbed into the definition of $\delta$) so that the CDW phase equals the difference between the ISDW phases.

The derivation of the spin and charge distributions is simplified by first assuming that the electron wavefunctions are plane-wave states. So we employ the creation and destruction operators for a d-band electron on site $i$ with spin $\sigma$:

$$\boldsymbol{\Psi}_i = \begin{pmatrix} a_{i\uparrow} \\ a_{i\downarrow} \\ b_{i\uparrow}^{(-)} \\ b_{i\downarrow}^{(-)} \\ b_{i\uparrow}^{(+)} \\ b_{i\downarrow}^{(+)} \end{pmatrix} \tag{A3}$$

which is a six-dimensional vector in band and spin space. While $a_{i\sigma}^{\dagger}$ and $a_{i\sigma}$ create and destroy electrons on band $a$ and site $i$, $b_{i\sigma}^{(\pm)\dagger}$ and $b_{i\sigma}^{(\pm)}$ create and destroy electrons on bands $b\pm$ and site $i$. These operators have the Fourier transforms

$$a_{\boldsymbol{k}\sigma} = \frac{1}{\sqrt{N}}\sum_i a_{i\sigma}\mathrm{e}^{-\mathrm{i}\boldsymbol{k}\cdot\boldsymbol{R}_i} \tag{A4$a$}$$

$$b_{\boldsymbol{k}\sigma}^{(+)} = \frac{1}{\sqrt{N}}\sum_i b_{i\sigma}^{(+)}\mathrm{e}^{-\mathrm{i}\boldsymbol{k}\cdot\boldsymbol{R}_i} \tag{A4$b$}$$

$$b_{\boldsymbol{k}\sigma}^{(-)} = \frac{1}{\sqrt{N}}\sum_i b_{i\sigma}^{(-)}\mathrm{e}^{-\mathrm{i}\boldsymbol{k}\cdot\boldsymbol{R}_i} \tag{A4$c$}$$

where $N$ is the number of atoms.

Then the spin and charge operators on site $i$ are given by

$$S_{iz} = \frac{\hbar}{2}\boldsymbol{\Psi}_i^{\dagger}\begin{pmatrix} \boldsymbol{\sigma}_z & \boldsymbol{\sigma}_z & \boldsymbol{\sigma}_z \\ \boldsymbol{\sigma}_z & \boldsymbol{\sigma}_z & \boldsymbol{\sigma}_z \\ \boldsymbol{\sigma}_z & \boldsymbol{\sigma}_z & \boldsymbol{\sigma}_z \end{pmatrix}\boldsymbol{\Psi}_i \tag{A5}$$

$$\varrho_i = \boldsymbol{\Psi}_i^{\dagger}\begin{pmatrix} \mathbf{1} & \mathbf{1} & \mathbf{1} \\ \mathbf{1} & \mathbf{1} & \mathbf{1} \\ \mathbf{1} & \mathbf{1} & \mathbf{1} \end{pmatrix}\boldsymbol{\Psi}_i \tag{A6}$$

where the polarization direction of the spin is taken along the $z$ axis. This axis is not related to the direction of the ordering wavevectors $\boldsymbol{Q}'_{\pm}$.

With the convention that repeated spin indices are summed, the expectation value of the spin is given by

$$\langle S_{iz}\rangle = \frac{\hbar}{2N}\sigma_{\mu\mu}^z\sum_{\boldsymbol{k}}\{\langle a_{\boldsymbol{k}\mu}^{\dagger}b_{\boldsymbol{k}\mu}^{(+)}\rangle\mathrm{e}^{-\mathrm{i}\boldsymbol{Q}'_+\cdot\boldsymbol{R}_i} + \langle a_{\boldsymbol{k}\mu}^{\dagger}b_{\boldsymbol{k}\mu}^{(-)}\rangle\mathrm{e}^{-\mathrm{i}\boldsymbol{Q}'_-\cdot\boldsymbol{R}_i} + \langle b_{\boldsymbol{k}\mu}^{(+)\dagger}a_{\boldsymbol{k}\mu}\rangle\mathrm{e}^{\mathrm{i}\boldsymbol{Q}'_+\cdot\boldsymbol{R}_i} + \langle b_{\boldsymbol{k}\mu}^{(-)\dagger}a_{\boldsymbol{k}\mu}\rangle\mathrm{e}^{\mathrm{i}\boldsymbol{Q}'_-\cdot\boldsymbol{R}_i}\}$$

$$\begin{aligned}
&= \overline{h}\frac{T}{N}\sum_{\boldsymbol{k},l}\{G^{ab+}_{\uparrow\uparrow}(\boldsymbol{k},\mathrm{i}\nu_l)\mathrm{e}^{-\mathrm{i}\boldsymbol{Q}'_+\cdot\boldsymbol{R}_i} + G^{ab-}_{\uparrow\uparrow}(\boldsymbol{k},\mathrm{i}\nu_l)\mathrm{e}^{-\mathrm{i}\boldsymbol{Q}'_-\cdot\boldsymbol{R}_i} \\
&\quad + G^{b+a}_{\uparrow\uparrow}(\boldsymbol{k},\mathrm{i}\nu_l)\mathrm{e}^{\mathrm{i}\boldsymbol{Q}'_+\cdot\boldsymbol{R}_i} + G^{b-a}_{\uparrow\uparrow}(\boldsymbol{k},\mathrm{i}\nu_l)\mathrm{e}^{\mathrm{i}\boldsymbol{Q}'_-\cdot\boldsymbol{R}_i}\} \\
&= -\frac{\overline{h}}{8\lambda}\left(\frac{V}{N}\right)\rho_{eh}g\{\mathrm{e}^{\mathrm{i}\phi_+-\mathrm{i}\boldsymbol{Q}'_+\cdot\boldsymbol{R}_i} + \mathrm{e}^{\mathrm{i}\phi_--\mathrm{i}\boldsymbol{Q}'_-\cdot\boldsymbol{R}_i} + \mathrm{e}^{-\mathrm{i}\phi_++\mathrm{i}\boldsymbol{Q}'_+\cdot\boldsymbol{R}_i} + \mathrm{e}^{-\mathrm{i}\phi_-+\mathrm{i}\boldsymbol{Q}'_-\cdot\boldsymbol{R}_i}\}
\end{aligned} \tag{A7}$$

which makes use of equation (A1) for $g$. So we finally find that

$$\langle S_{iz}\rangle = -\frac{\overline{h}}{2\lambda}\left(\frac{V}{N}\right)\rho_{eh}g\hat{\boldsymbol{m}}(-1)^{2R_z/a}\cos\phi_{av}\cos\left(\frac{2\pi}{a}\partial' R_z - \frac{\theta}{2}\right) \tag{A8}$$

which can be rewritten as equation (3) in the text after the Bloch functions are reinstated. Notice that the Matsubara summation must precede the $\boldsymbol{k}$ integral so that the operators are evaluated at equal times.

The ICDW can be written as

$$\begin{aligned}
\langle\varrho_i\rangle &= \langle b^{(+)\dagger}_{i\mu}b^{(-)}_{i\mu}\rangle + \langle b^{(-)\dagger}_{i\mu}b^{(+)}_{i\mu}\rangle \\
&= \frac{1}{N}\sum_{\boldsymbol{k}}\{\langle b^{(-)\dagger}_{\boldsymbol{k}\mu}b^{(+)}_{\boldsymbol{k}\mu}\rangle\mathrm{e}^{-\mathrm{i}(\boldsymbol{Q}'_+-\boldsymbol{Q}'_-)\cdot\boldsymbol{R}_i} + \langle b^{(+)\dagger}_{\boldsymbol{k}\mu}b^{(-)}_{\boldsymbol{k}\mu}\rangle\mathrm{e}^{\mathrm{i}(\boldsymbol{Q}'_+-\boldsymbol{Q}'_-)\cdot\boldsymbol{R}_i}\} \\
&= 2\frac{T}{N}\sum_{\boldsymbol{k},l}\{G^{b-b+}_{\uparrow\uparrow}(\boldsymbol{k},\mathrm{i}\nu_l)\mathrm{e}^{-\mathrm{i}(\boldsymbol{Q}'_+-\boldsymbol{Q}'_-)\cdot\boldsymbol{R}_i} + G^{b+b-}_{\uparrow\uparrow}(\boldsymbol{k},\mathrm{i}\nu_l)\mathrm{e}^{\mathrm{i}(\boldsymbol{Q}'_+-\boldsymbol{Q}'_-)\cdot\boldsymbol{R}_i}\} \\
&= -\frac{\delta}{2\lambda'}\left(\frac{V}{N}\right)\rho_{eh}\cos\left(\frac{4\pi}{a}\partial' R_z - \psi\right)
\end{aligned} \tag{A9}$$

which uses the self-consistent expression of equation (A2) for $\delta$. When the Bloch functions replace the plane-wave states, equation (A9) becomes equation (4) in the text.

## References


[1] The properties of Cr alloys are reviewed by
Fawcett E, Alberts H L, Galkin V Yu, Noakes D R and Yakhmi J V 1994 *Rev. Mod. Phys.* **66** 26
In particular, this comprehensive work contains all of the references on CrFe and CrSi alloys.

[2] Fedders P A and Martin P C 1966 *Phys. Rev.* **143** 8245

[3] Lomer W M 1962 *Proc. Phys. Soc.* **80** 489

[4] Fishman R S and Liu S H 1993 *Phys. Rev.* B **48** 3820

[5] Tsunoda Y, Mori M, Kunitomi N, Teraoka Y and Kanamori J 1974 *Solid State Commun.* **14** 287

[6] Prekul A F and Sudareva S V 1979 *Phys. Met. Metallogr.* **46** 46

[7] Pynn R, Press W, Shapiro S M and Werner S A 1976 *Phys. Rev.* B **13** 295

[8] Iida S, Khono M, Tsunoda Y and Kunitomi N 1981 *J. Phys. Soc. Japan* **50** 2581

[9] Hill J P, Hegelsen G and Gibbs D 1995 *Phys. Rev.* B **51** 10 336

[10] Young C Y and Sokoloff J B 1974 *J. Phys. F: Met. Phys.* **4** 1304

[11] Asano S and Yamashita J 1967 *J. Phys. Soc. Japan* **23** 714

[12] Rath J and Callaway J 1973 *Phys. Rev.* B **8** 5398

[13] Shibatani A, Motizuki K and Nagamiya T 1969 *Phys. Rev.* **177** 984

[14] Fishman R S and Liu S H 1994 *Phys. Rev.* B **49** 3308

[15] Mori M and Tsunoda Y 1993 *J. Phys. C: Solid State Phys.* **5** L77

[16] Nakajima S and Kurihara Y 1975 *J. Phys. Soc. Japan* **38** 330

[17] Overhauser A W 1968 *Phys. Rev.* **167** 691

[18] Kulikov N I and Kulatov E T 1982 *J. Phys. F: Met. Phys.* **12** 2291 and references therein

[19] A residual ICDW $\delta/\lambda' \propto g^2/T_N^*$ survives even as $\lambda' \to 0$. The remnant correlation between the $b+$ holes and $b-$ electrons is induced through their coupling with the SDW. However, in the $\lambda' \to 0$ limit, the residual ICDW has no effect on the thermodynamics of the I phase.

[20] Jiang X W and Fishman R S, unpublished
[21] Fishman R S and Liu S H 1992 *Phys. Rev.* B **45** 12 306
[22] Ishikawa Y, Tournier R and Filippi J 1965 *J. Phys. Chem. Solids* **26** 1727
[23] Suzuki T 1966 *J. Phys. Soc. Japan* **21** 442
[24] Nakanishi K and Kasuya T 1977 *J. Phys. Soc. Japan* **42** 833
[25] Cable J W 1977 *J. Magn. Magn. Mater.* **5** 112
[26] Fawcett E, private communication